Supporting Information for

Facile synthesis and self-assembly of multihetero-arm hyperbranched polymers brushes

Chao Gao,[1*] and Xing Zheng[2]

[1] *Key Laboratory of Macromolecular Synthesis and Functionalization (Ministry of Education), Department of Polymer Science and Engineering, Zhejiang University, 38 Zheda Road, Hangzhou 310027, P. R. China.*

[2] *College of Chemistry and Chemical Engineering, Shanghai Jiao Tong University, 800 Dongchuan Road, Shanghai 200240, P. R. China.*

[*] To whom correspondence should be addressed. E-mail: chaogao@zju.edu.cn.

List of Supporting Information

ESI1. Kinetics of self-condensing atom transfer radical polymerization of click-inimer **3**

ESI2. Additional AFM images of bihetero-arm hyperbranched polymer brush

ESI3. Dynamic light scattering (DLS) results for the bihetero-arm hyperbranched polymer brush

ESI4. SEM images of assembled micelles of the bihetero-arm hyperbranched polymer brush

ESI5. Optical microscope images of the trinity brush in DMF/H_2O

ESI6. SEM images of assembled structures of the trinity brush

ESI7. TEM images of assembled structures of the trinity brush

ESI8. ^{1}H NMR spectra of the trinity brush in the mixed solvent of DMF-d_7 and D_2O

ESI1. Kinetics of self-condensing atom transfer radical polymerization of AzBrMA (3)

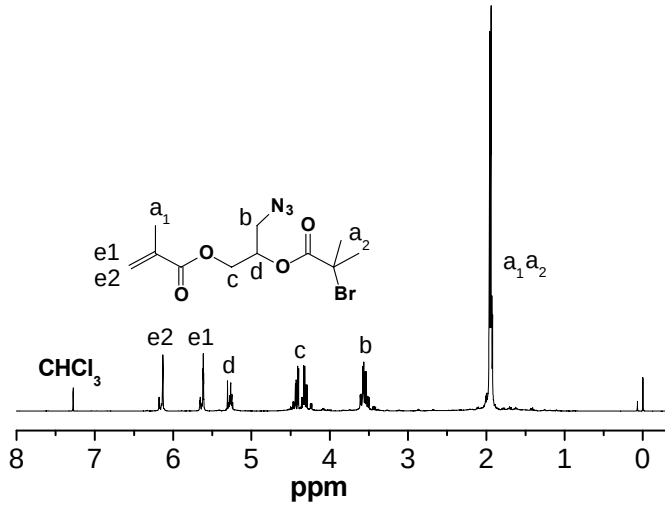

Figure S1. ^{1}H NMR spectrum of clickable-inimer **3**, AzBrMA.

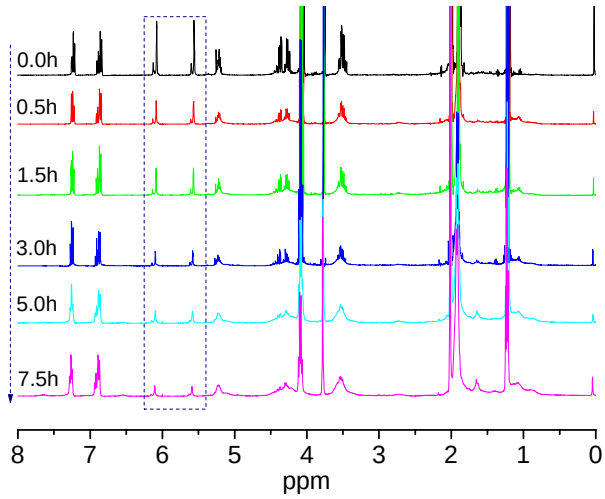

Figure S2. ^{1}H NMR spectra of the samples taken from the reaction system at given times for the SC-ATRP of AzBrMA with the reference of anisole, showing the decrease of vinyl peaks and increase of methyl protons.

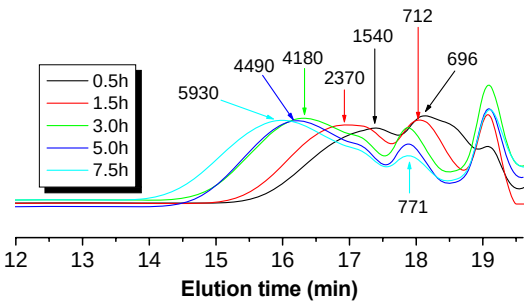

Figure S3. GPC curves of the samples taken from the reaction system at given times for the SC-ATRP of AzBrMA, showing (1) the polydispersity index (PDI) of the species is quite broad, (2) the molar mass of the main peak increases with the reaction time or conversion, and (3) various species with different molar mass covered from macromolecules, oligomers, and dimmers are existed in the system.

ESI2. Additional AFM images of bihetero-arm hyperbranched polymer brush 5

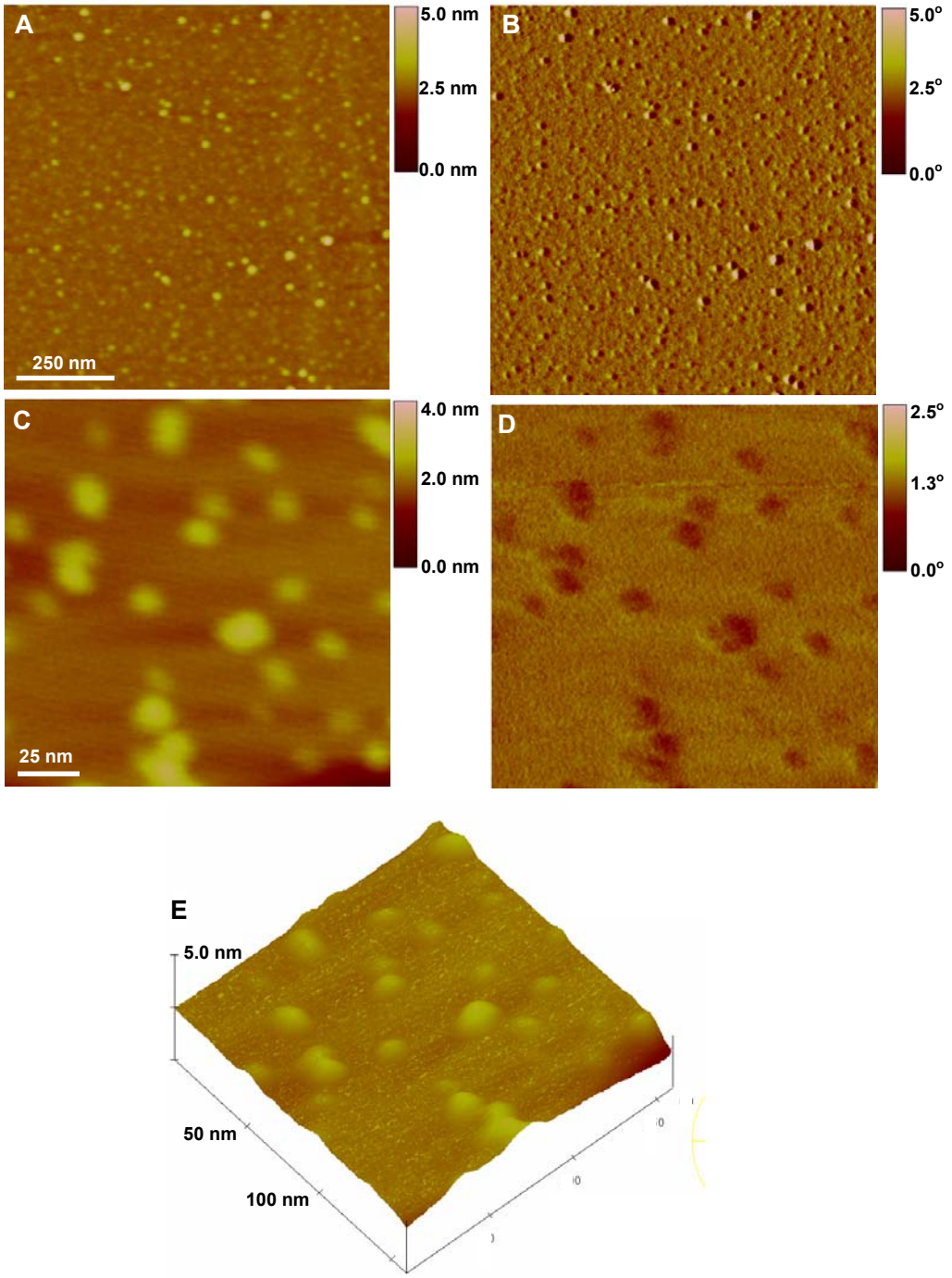

Figure S4. Height (A, C)and phase (B, D) AFM images of bihetero-arm hyperbranched polymer brush **5** from diluted DMF solution (0.01 mg/mL). E: 3D diagram of C image. These images show the morphology of individual macromolecules of globular hyperbranched polymer brushes.

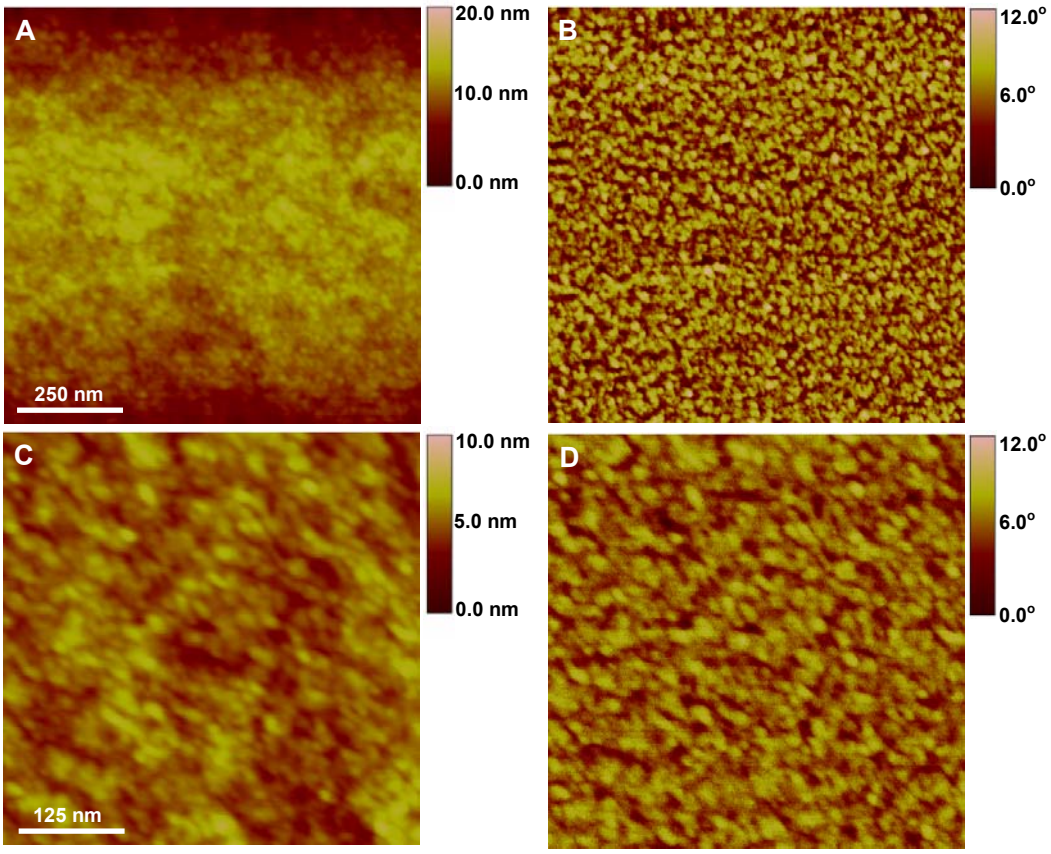

Figure S5. Height (A,C)and phase (B, D) AFM images of bihetero-arm hyperbranched polymer brush **5** from high concentration of DMF solution (1 mg/mL). These images show the morphology of macromolecular film morphology of globular hyperbranched polymer brushes.

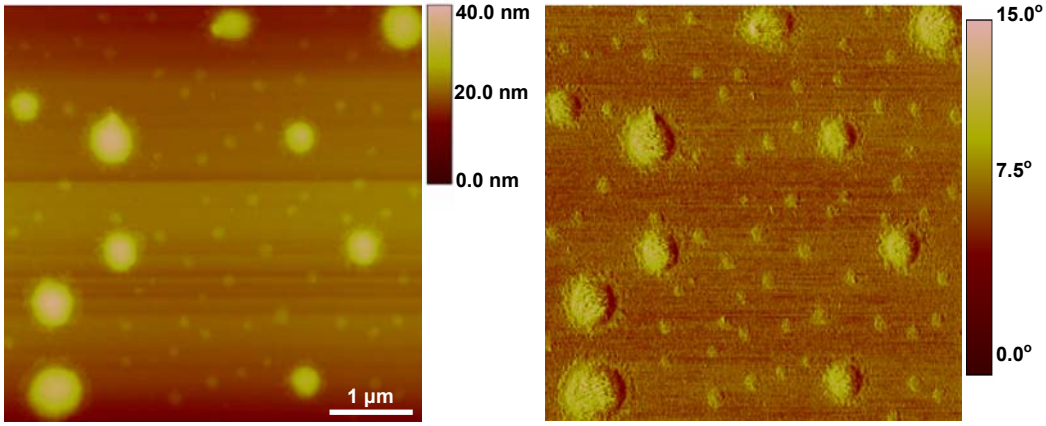

Figure S6. Height (left)and phase (right) AFM images of bihetero-arm hyperbranched polymer brush **5** after addition of tiny amount of water into its DMF solution, showing that the macromolecules start to self-assemble into globular micelles from the binary unimolecular brushes.

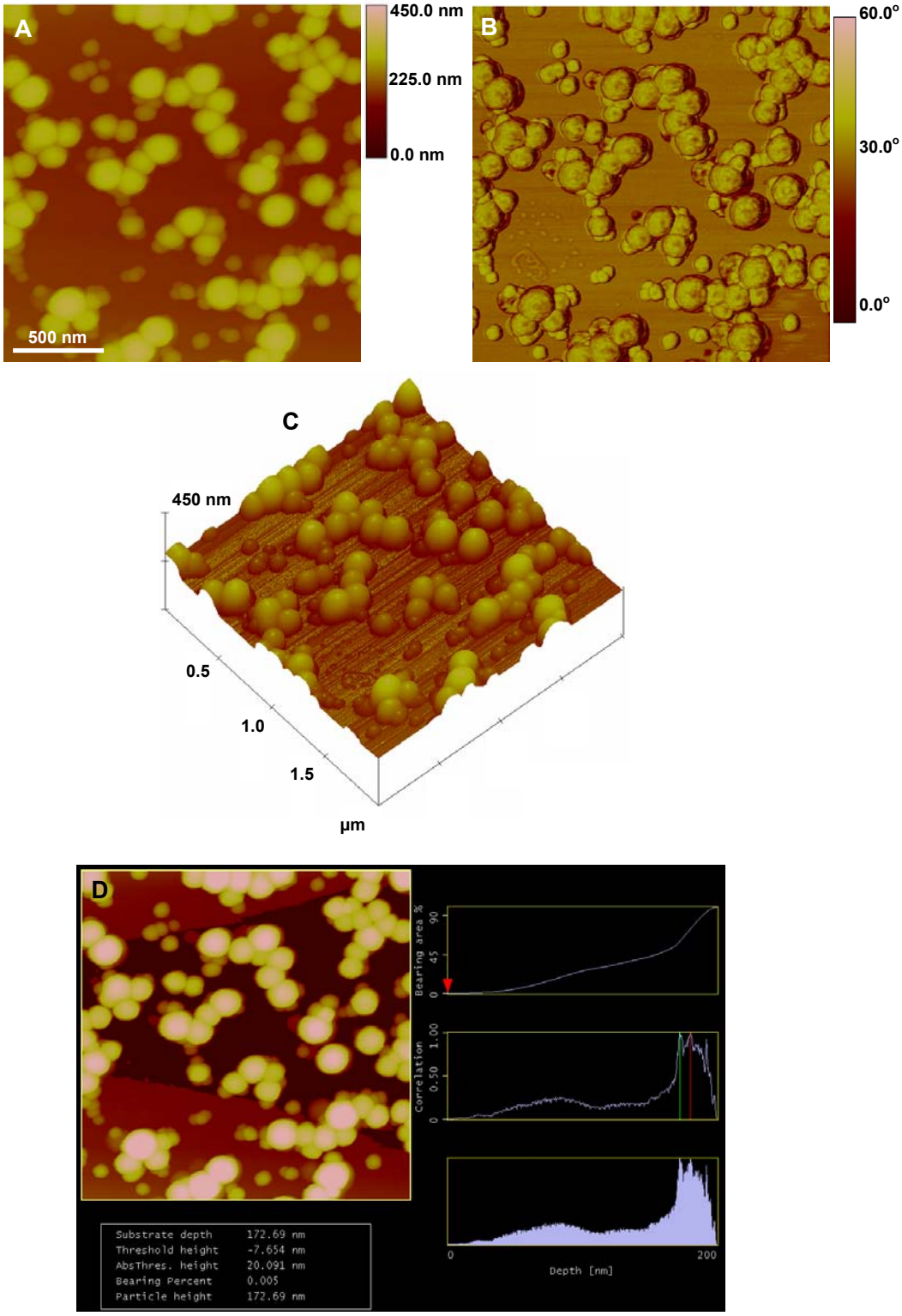

Figure S7. Height (A), phase (B) and 3D (C) images of self-assembled spherical particles of bihetero-arm hyperbranched polymer brush **5** in DMF/H_2O (2/1 by volume). D: particle analysis of image A. The average particle height is ca. 172 nm.

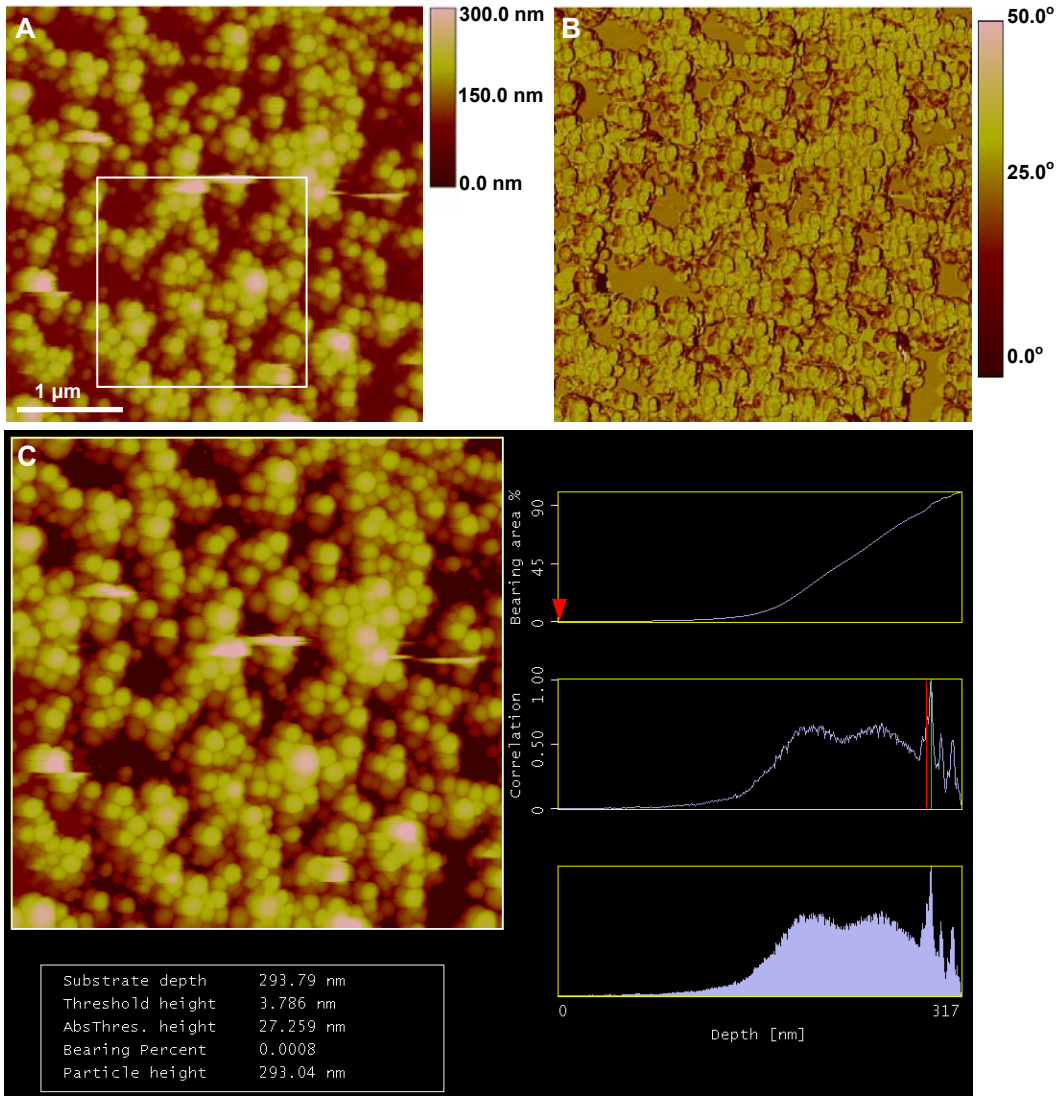

Figure S8. More height (A) and phase (B) images of self-assembled spherical particles of bihetero-arm hyperbranched polymer brush **5** in DMF/H_2O (2/1 by volume) in a larger area. C: particle analysis of image A. The average particle height is ca. 293 nm due to the aggregation of assembled micelles. The white square area of A will be zoomed in as shown in Figure S9.

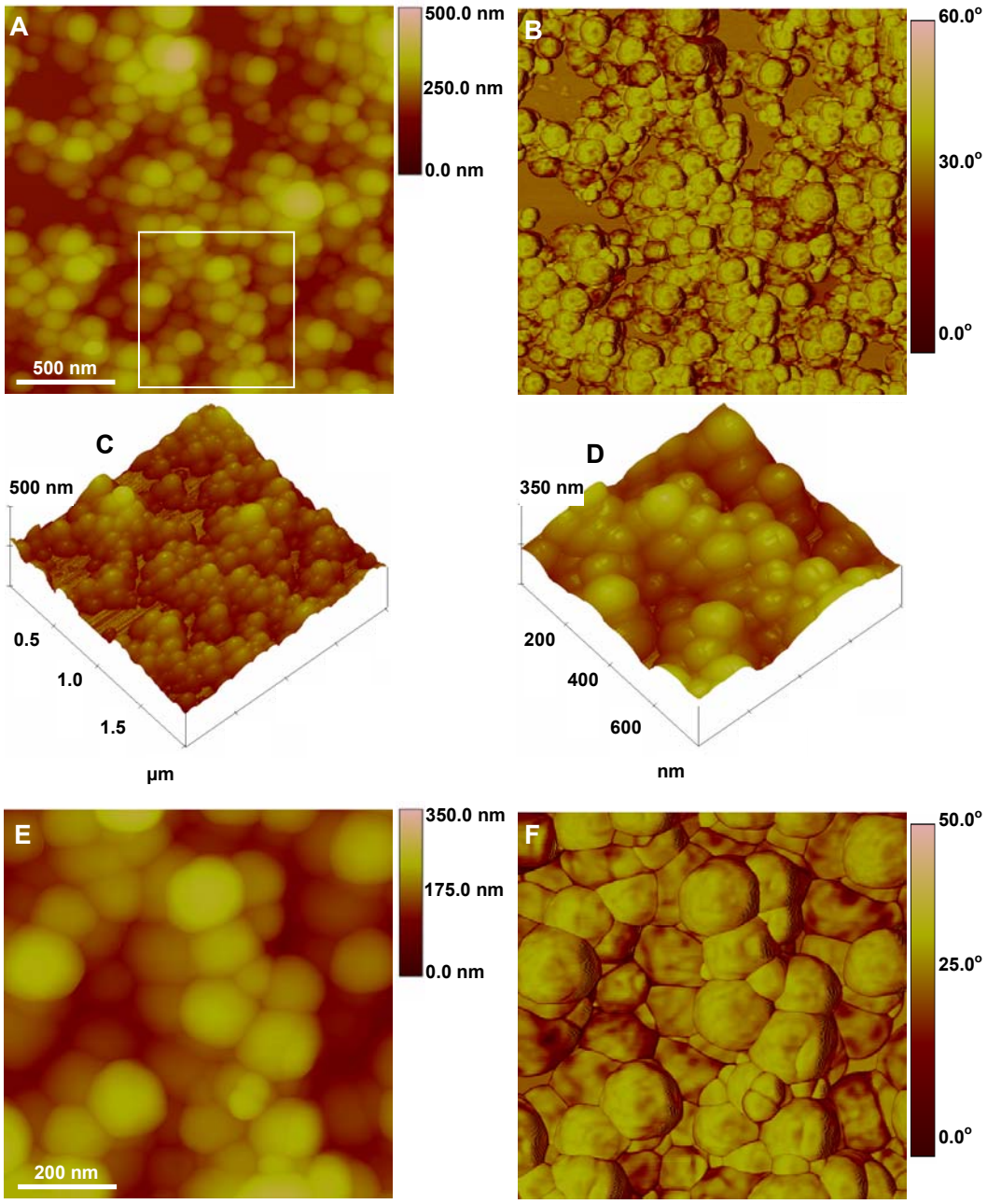

Figure S9. Zoomed in height (A, E) and phase (B, F) images of self-assembled spherical particles of bihetero-arm hyperbranched polymer brush **5** in DMF/H_2O (2/1 by volume). C, D: 3D diagrams of images A and E, respectively, showing the compact spherical structures of assembled micelles.

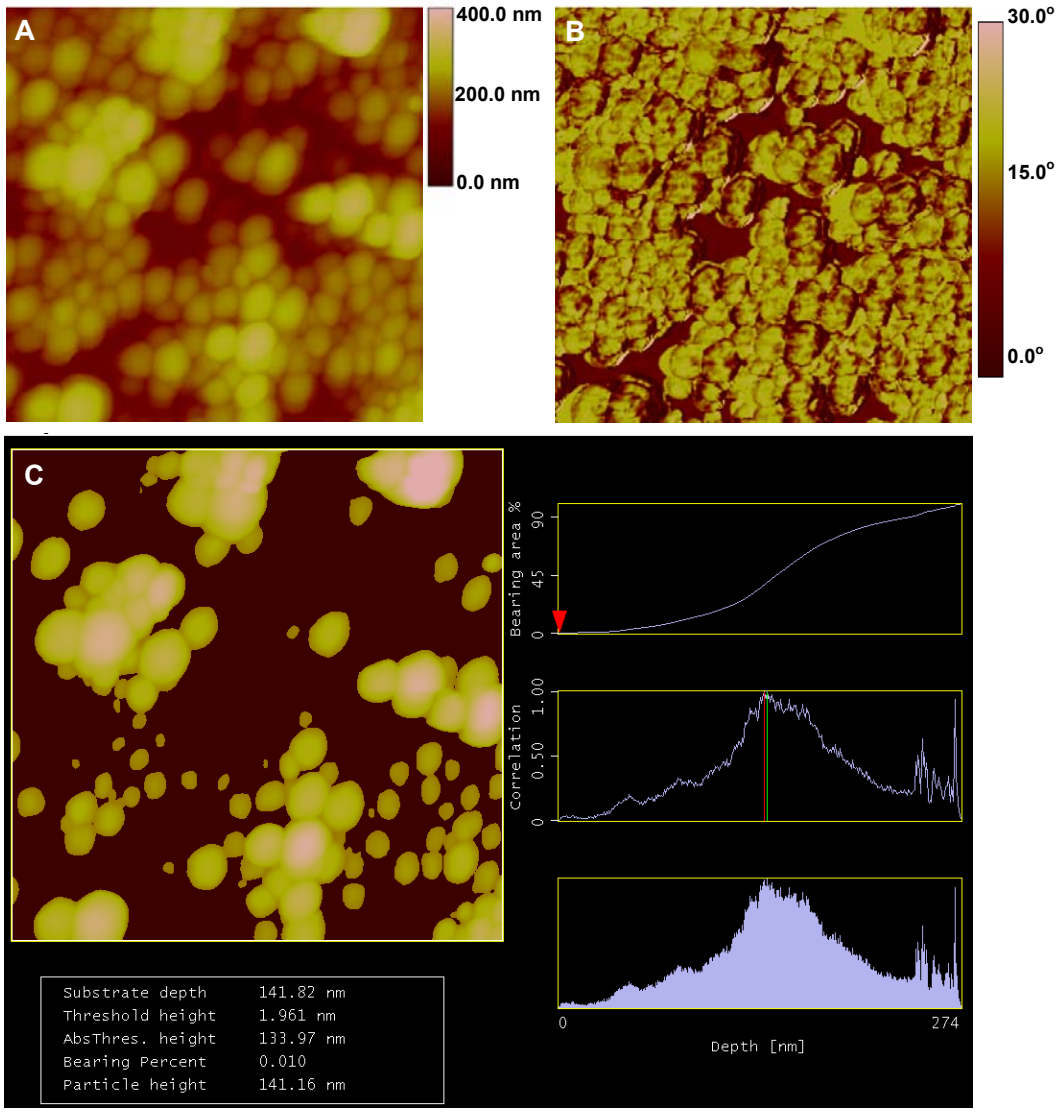

Figure S10. Height (A) and phase (B) images of self-assembled spherical particles of bihetero-arm hyperbranched polymer brush **5** in DMF/H_2O (10/1 by volume). C: particle analysis of image A. The average particle height is ca. 141 nm, slightly smaller than those obtained in DMF/H_2O (2/1 by volume) shown above (Figures S11-13).

ESI3. Dynamic light scattering (DLS) results for the bihetero-arm hyperbranched polymer brush

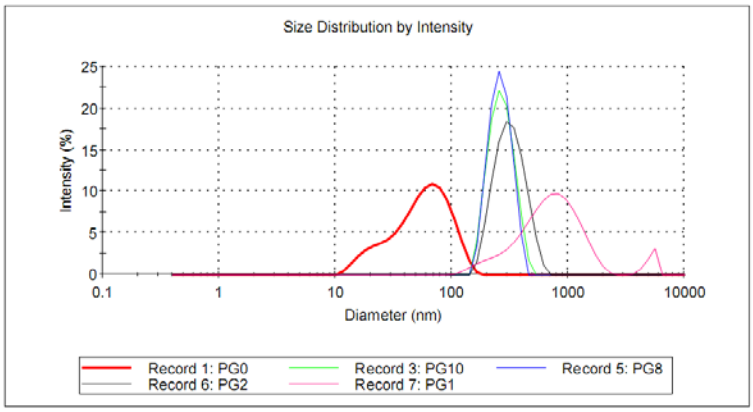

Figure S11. Dynamic light scattering results for the bihetero-arm hyperbranched polymer brush **5** in DMF solution with the addition of no water (red, Record 1), 1/10 water (green, Record 3), 1/8 water (blue, Record 5), 1/2 water (light gray, Record 6), and 1/1 water (pink, Record 7).

The corresponding particle sizes are listed below.

H_2O/DMF(mL/mL)	Z-Average (nm)	PDI	Diameter (nm)	Width (nm)
0	60.32	0.288	60.86	30.81
1/10	256.9	0.046	271.7	65.89
1/8	253.6	0.018	264.3	57.23
1/2	299.1	0.074	324.5	94.86
1/1	652.2	0.429	1260	1201

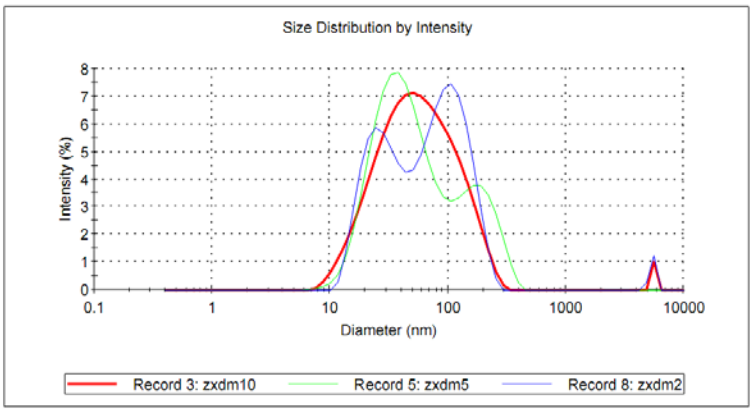

Figure S12. Dynamic light scattering results for the bihetero-arm hyperbranched polymer brush **5** in DMF solution with the addition of 1/10 methanol (red, Record 3), 1/5 methanol (green, Record 5), and 1/2 methanol (blue, Record 8).

The corresponding particle sizes are listed below.

CH_3OH/DMF(mL/mL)	Z-Average (nm)	PDI	Diameter (nm)	Width (nm)
0	60.32	0.288	60.86	30.81
1/10	60.68	0.249	68.41	50.42
1/5	67.94	0.234	44.41, 186.6	23.72, 65.88
1/2	53.77	0.441	103.4, 27.37, 5422	45.25, 8.91, 292.1

ESI4. SEM images of assembled micelles of the bihetero-arm hyperbranched polymer brush

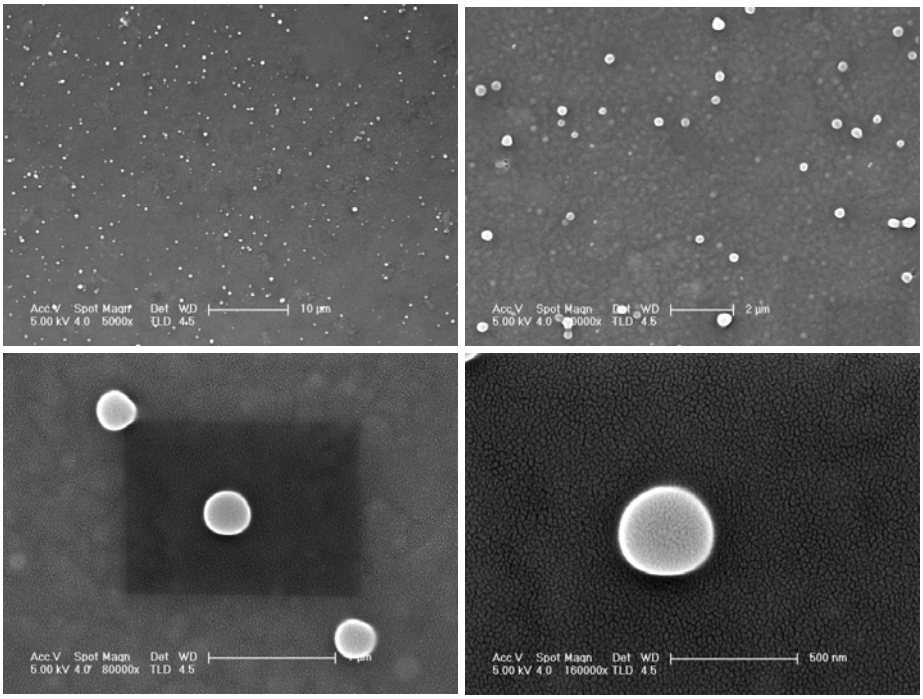

Figure S13. Representative SEM images of assembled micelle particles of the bihetero-arm hyperbranched polymer brush **5** at different amplification, showing the particles have diameters of ca. 250-300 nm.

ESI5. Optical microscope images of trinity polymer brush in DMF/H_2O

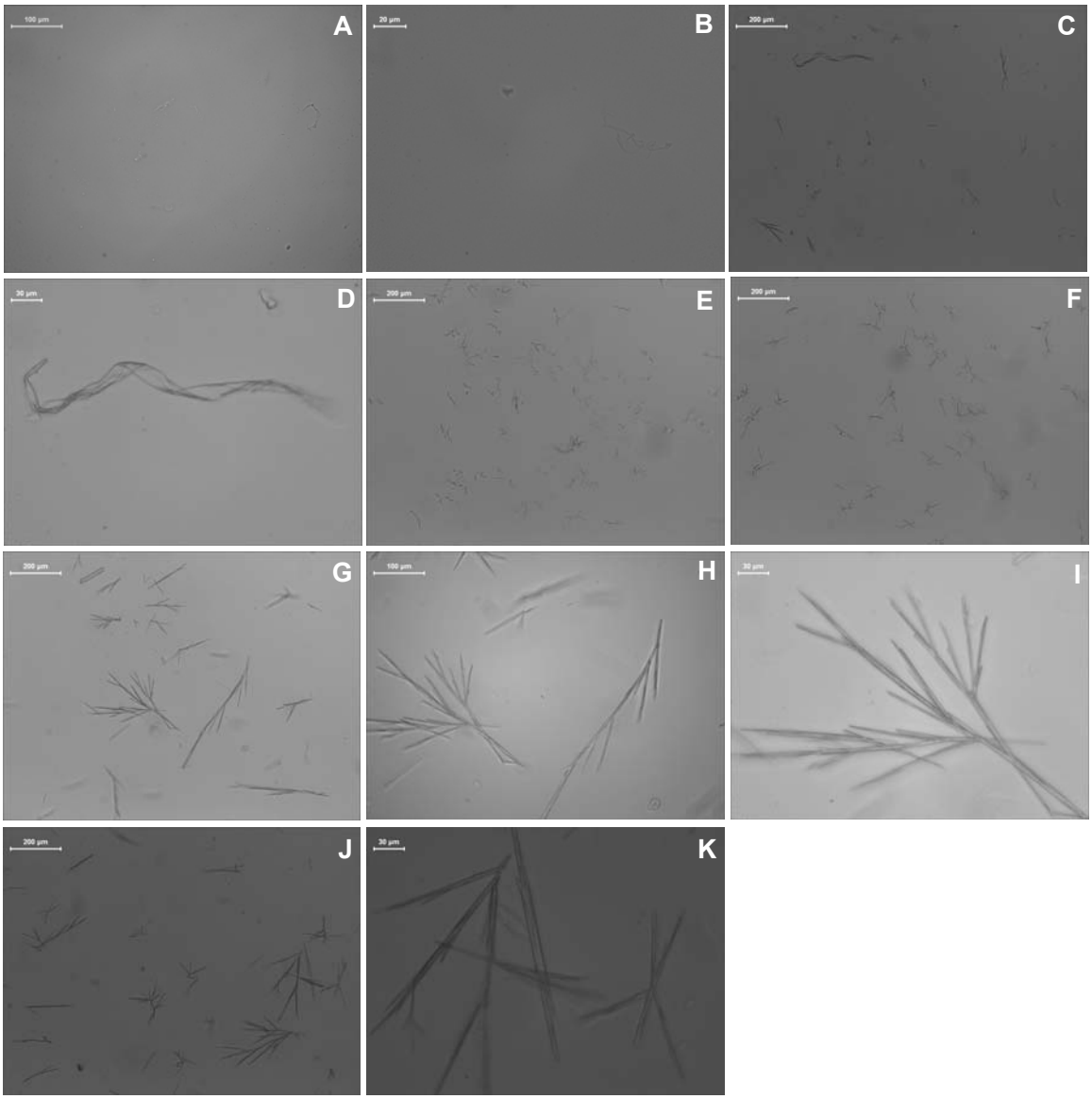

Figure S14. Optical microscope images of trinity brush **8** in DMF/water (2/1 by volume) for 15 min (A), 1 h (B), 3 h (C, D), 4 h (E, F), and 24 h (G-K).

ESI6. SEM images of assembled structures of hyperbranched trinity brush

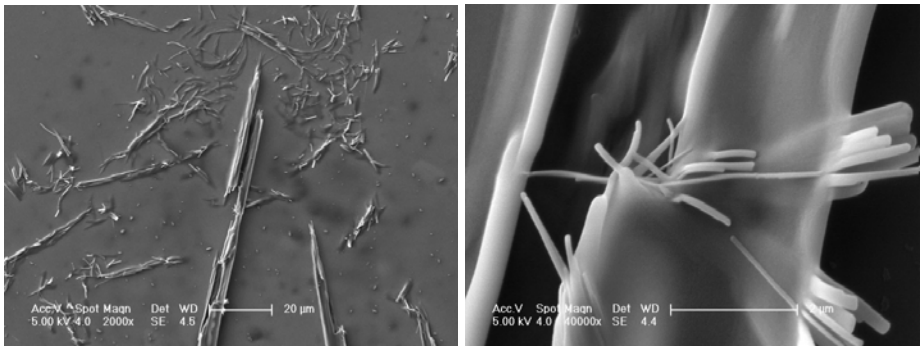

Figure S15. Selected SEM images of assembled structures of the trinity brush **8**, showing the unclosed tubes and branching sites.

ESI7. TEM images of assembled structures of the trinity brush

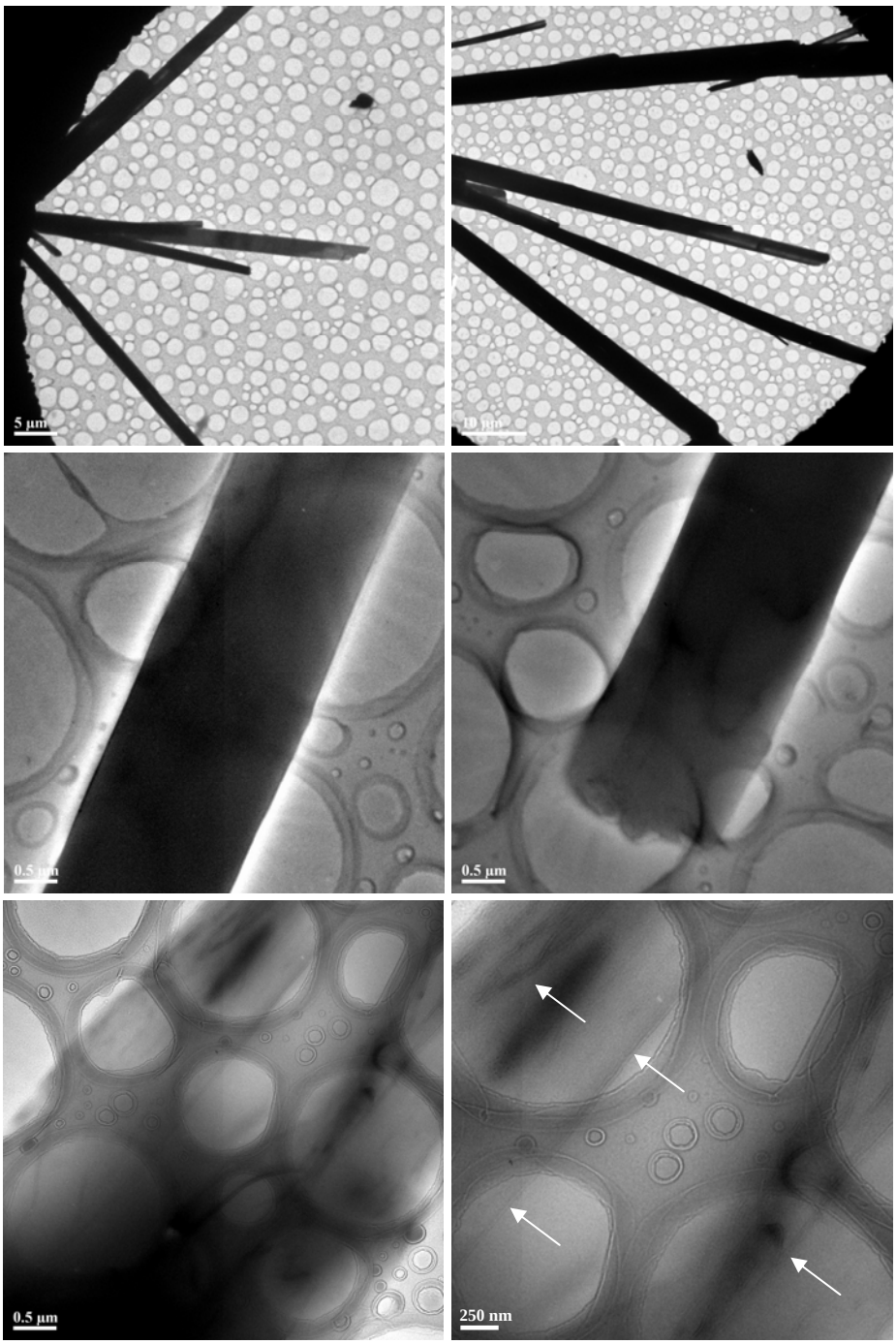

Figure S16. Representative TEM images of assembled structures of the trinity brush **8**, showing the straight big tubes at low amplification and fine structures composed of parallel-aligned small fibers at high amplification (see arrows).

ESI8. ^{1}H NMR spectra of the trinity brush in the mixed solvent of DMF-d_7 and D_2O

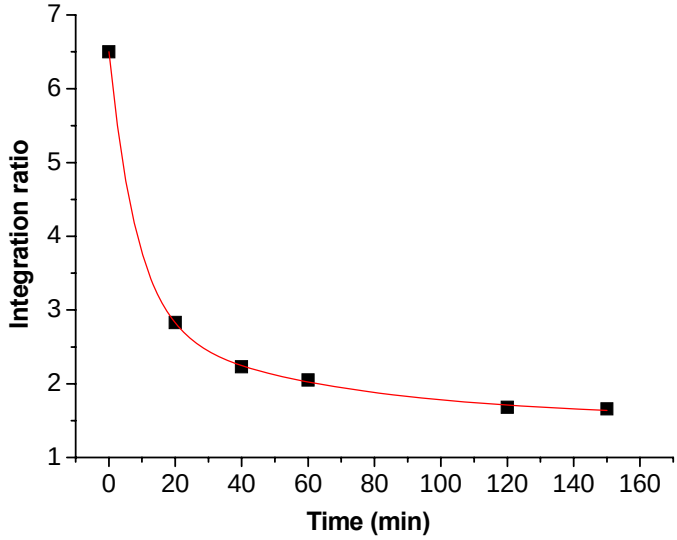

Figure S17. The integration ratio of hydrophobic arms of C16 and PtBA to hydrophilic arms of PEG for the trinity brush **8** in the mixed solvent of DMF-d_7 and D_2O as a function of time after the addition of D_2O into DMF-d_7 solution of YYB2. It shows the exponential decrease tendency for the ratio, indicating that (1) the self-assembly process is dynamic, and (2) the hydrophobic arms tend to be covered gradually by the hydrophilic ones with the assembly going further.

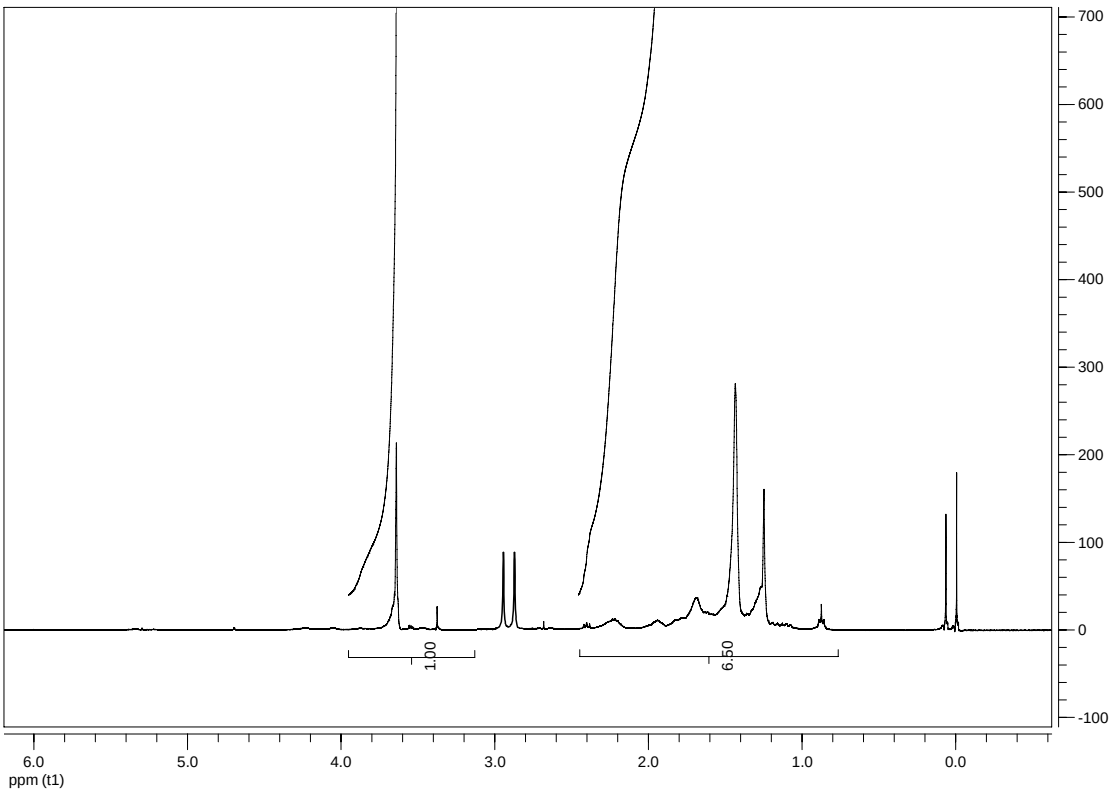

Figure S18. ^{1}H NMR spectrum of the trinity brush **8** in the solvent of DMF-d_7, showing clearly the proton peaks of C16 and P*t*BA arms during 2.4-0.8 ppm.

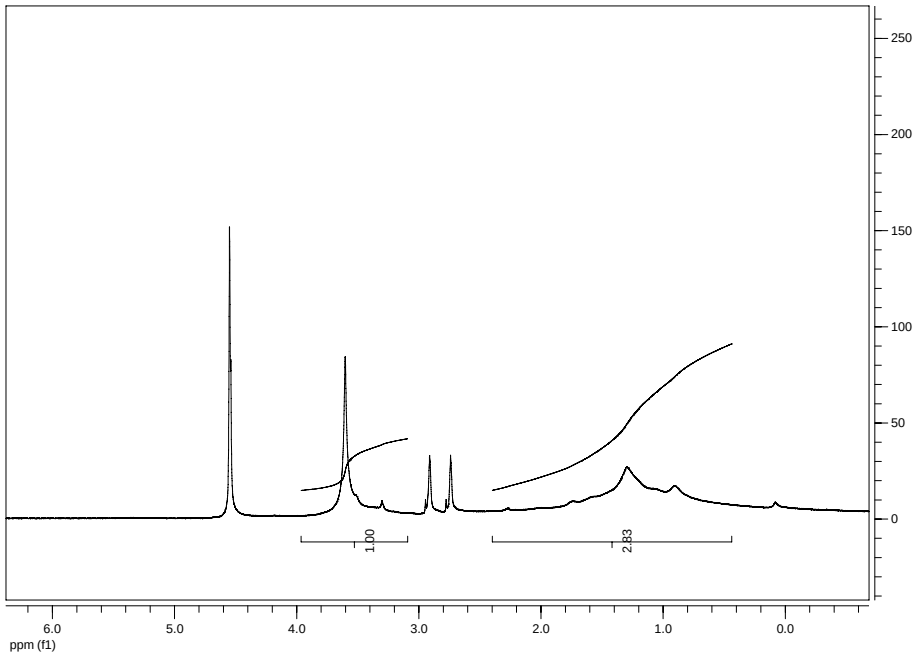

Figure S19. ^{1}H NMR spectrum of the trinity brush in the mixed solvent of DMF-d_7 and D_2O (2:1 by volume) after addition of D_2O into DMF-d_7 for 20 min, showing the overlapped proton peaks of C16 and P*t*BA arms during 2.4-0.8 ppm. The PEG proton peak at 3.6 ppm is still clearly observed.

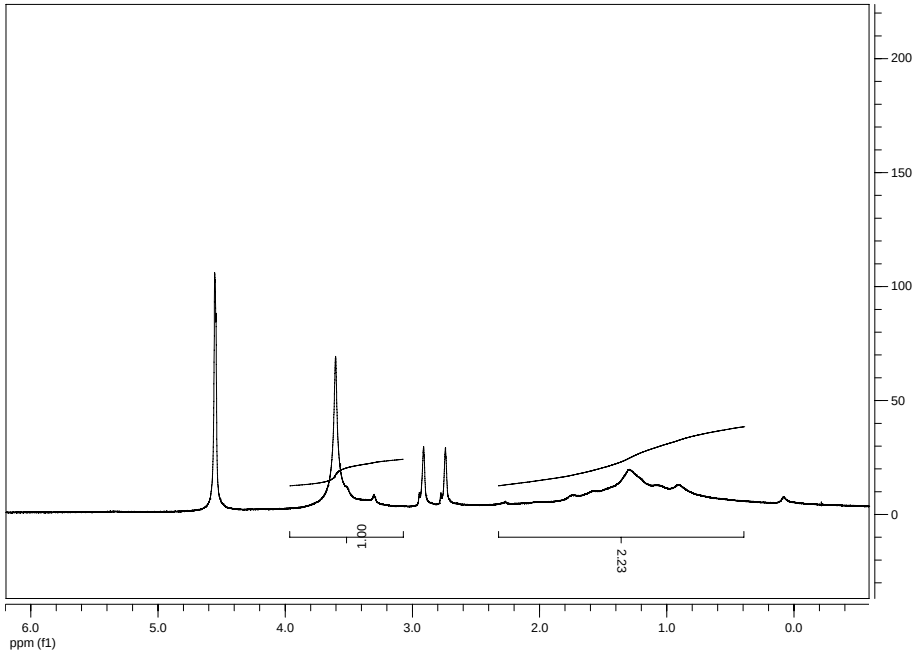

Figure S20. ^{1}H NMR spectrum of the trinity brush in the mixed solvent of DMF-d_7 and D_2O (2:1 by volume) after addition of D_2O into DMF-d_7 for 40 min, showing the overlapped proton peaks of C16 and P*t*BA arms during 2.4-0.8 ppm. The PEG proton peak at 3.6 ppm is still clearly observed.

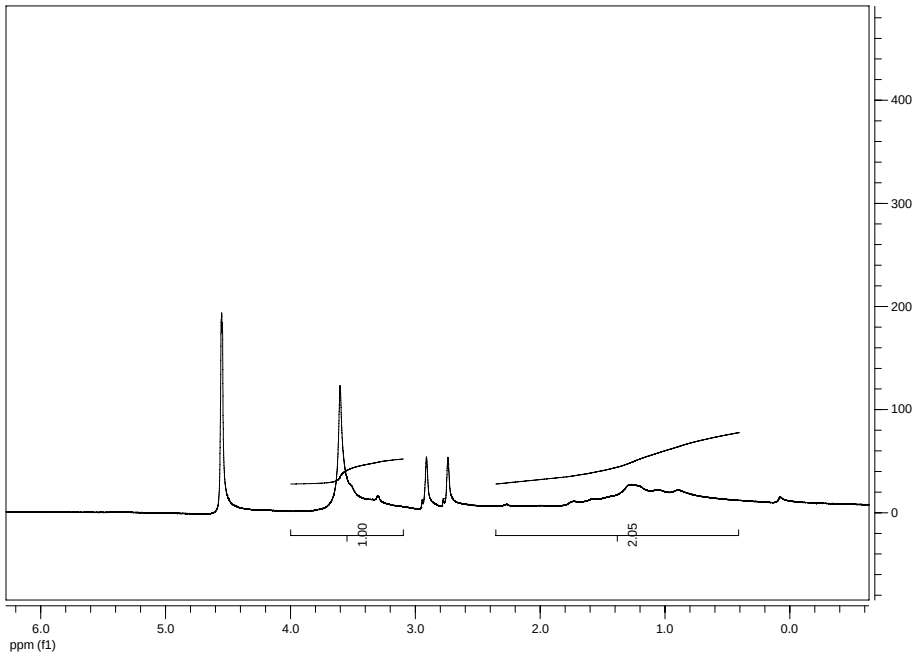

Figure S21. ^{1}H NMR spectrum of the trinity brush in the mixed solvent of DMF-d_7 and D_2O (2:1 by volume) after addition of D_2O into DMF-d_7 for 60 min, showing the overlapped proton peaks of C16 and P*t*BA arms during 2.4-0.8 ppm. The PEG proton peak at 3.6 ppm is still clearly observed.

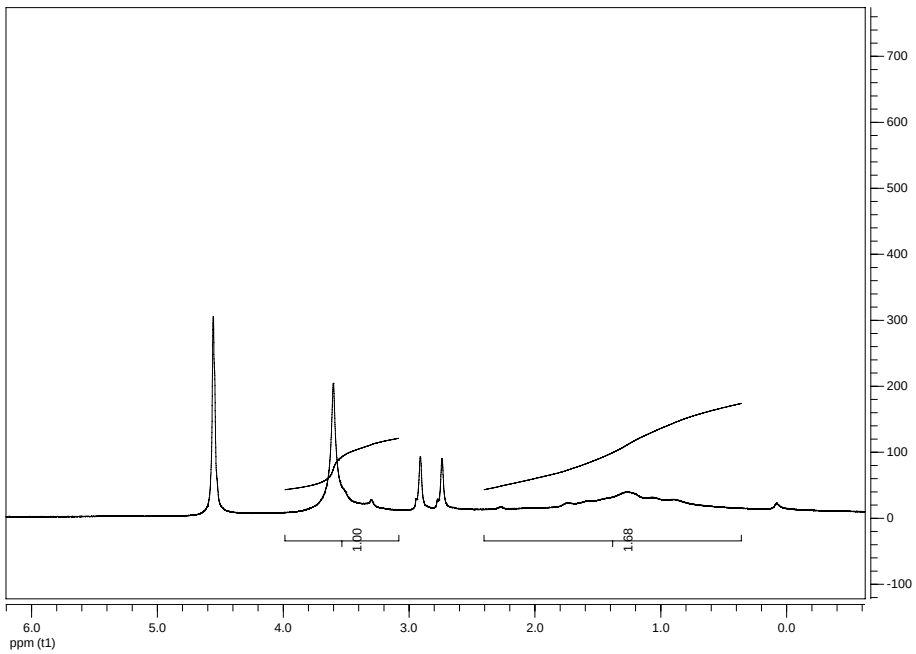

Figure S22. ^{1}H NMR spectrum of the trinity brush in the mixed solvent of DMF-d_7 and D_2O (2:1 by volume) after addition of D_2O into DMF-d_7 for 120 min. The overlapped proton peaks of C16 and P*t*BA arms during 2.4-0.8 ppm are almost flattened. The PEG proton peak at 3.6 ppm is still clearly observed.

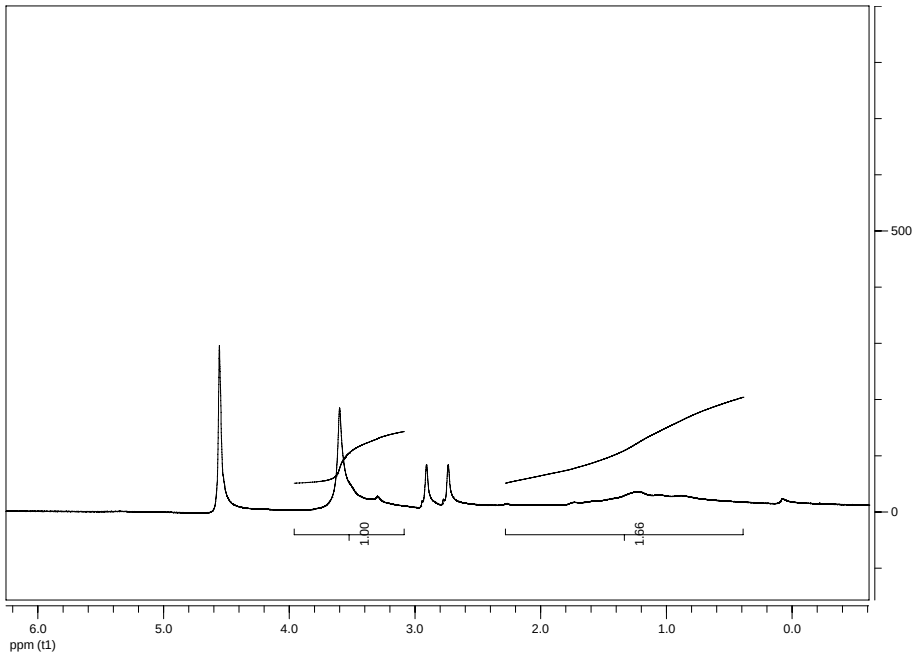

Figure S23. ^{1}H NMR spectrum of the trinity brush in the mixed solvent of DMF-d_7 and D_2O (2:1 by volume) after addition of D_2O into DMF-d_7 for 150 min. The overlapped proton peaks of C16 and P*t*BA arms during 2.4-0.8 ppm are hardly observed. The PEG proton peak at 3.6 ppm is still clearly observed with an obvious broadening effect.